[redacted]

Copy
RM L57

NACA

RESEARCH MEMORANDUM

EXPERIMENTAL DETERMINATION OF DAMPING IN PITCH OF SWEPT AND DELTA WINGS AT SUPERSONIC MACH NUMBERS

By John A. Moore

Langley Aeronautical Laboratory
Langley Field, Va.

NATIONAL ADVISORY COMMITTEE FOR AERONAUTICS

WASHINGTON

September 19, 1957

[redacted]

 [redacted]

NATIONAL ADVISORY COMMITTEE FOR AERONAUTICS

RESEARCH MEMORANDUM

EXPERIMENTAL DETERMINATION OF DAMPING IN PITCH OF SWEPT AND DELTA WINGS AT SUPERSONIC MACH NUMBERS

By John A. Moore

SUMMARY

The damping-in-pitch derivative $C_{m_q} + C_{m_{\dot{\alpha}}}$ was determined experimentally at Mach numbers of 2.96 and 3.92 for two delta wings having aspect ratios of 2 and 3 and for one sweptback tapered wing having an aspect ratio of 3 by using a free-oscillation technique. The tests were made at Reynolds numbers based on mean aerodynamic chord from 4×10^6 to 12×10^6 for an angle-of-attack range of 0° to 10°. The reduced-frequency parameter $\frac{\omega \bar{c}}{2V}$ ranged from 0.006 to 0.022.

The damping increased with increasing angle of attack, but the changes in damping with variation of Reynolds number and pitching-center location were within the accuracy of the data. The variation of damping with oscillation frequency was not noticeable for the delta wings; but, for the sweptback tapered wing, the damping was much lower for the high oscillation frequency. The values of damping derivatives for the delta wings were about 15 percent below those predicted by linear theory at zero angle of attack for each Mach number.

INTRODUCTION

The linearized supersonic-flow theory has been used by many investigators to determine the longitudinal dynamic-stability derivatives C_{m_q} and $C_{m_{\dot{\alpha}}}$ for triangular wings and sweptback tapered wings (refs. 1 to 4). Since it is difficult to isolate C_{m_q} and $C_{m_{\dot{\alpha}}}$ in experimental tests, most of the published data are on the dynamic stability derivative $C_{m_q} + C_{m_{\dot{\alpha}}}$. Reference 5 presents data on delta and sweptback tapered wings with body at Mach numbers up to 1.9. Reference 6 gives data for

[redacted]

delta wings with body at Mach numbers to 2.41. For a delta wing alone, reference 7 shows the use of a side-wall-mounted model to obtain data at Mach numbers up to 2.0. The purpose of the present investigation is to obtain $C_{m_q} + C_{m_{\dot{\alpha}}}$ at higher Mach numbers for delta and sweptback tapered wings alone and to determine the effects of angle of attack, Reynolds number, oscillation frequency, and location of pitching center on the stability derivative $C_{m_q} + C_{m_{\dot{\alpha}}}$.

Two delta wings having aspect ratios of 2 and 3 and one sweptback tapered wing having an aspect ratio of 3 were tested at Mach numbers of 2.96 and 3.92 by using a free-oscillation technique. The test Reynolds numbers based on mean aerodynamic chord were 4×10^6 and 6.8×10^6 for the sweptback tapered wing, 4.9×10^6 and 8.0×10^6 for the delta wing having an aspect ratio of 3, and 7.4×10^6 and 12.0×10^6 for the delta wing having an aspect ratio of 2. The reduced-frequency parameters were approximately 0.006 and 0.011 for the sweptback tapered wing, 0.008 and 0.015 for the delta wing having an aspect ratio of 3, and 0.011 and 0.022 for the delta wing having an aspect ratio of 2.

SYMBOLS

A	aspect ratio, $\frac{b^2}{S}$ or $\frac{2b}{c_r(1 + \lambda)}$
b	wing span
c_r	root chord
$\bar{c}$	mean aerodynamic chord, $\frac{2}{3}c_r$ for delta wings; $\frac{2}{3}c_r\left(\frac{\lambda^2 + \lambda + 1}{\lambda + 1}\right)$ for sweptback tapered wings
d	distance from wing apex to center of rotation
D	damping moment due to angular velocity
I	moment of inertia
K	mechanical spring constant
M	Mach number
q	angular velocity in pitch, radians/sec
R	Reynolds number

S wing area

t time

V velocity

α angle of attack of wing center line with respect to free-stream direction

ρ density

θ amplitude of oscillation

θ_0 value of θ at $t = 0$

ω frequency, radians/sec

$\frac{\omega \bar{c}}{2V}$ reduced-frequency parameter

C_m pitching-moment coefficient, $\frac{\text{Pitching moment}}{\frac{1}{2}\rho V^2 S\bar{c}}$

$C_{m_\alpha} = \frac{\partial C_m}{\partial \alpha}$

$C_{m_q} = \frac{\partial C_m}{\partial \frac{q\bar{c}}{2V}}$

$C_{m_{\dot{\alpha}}} = \frac{\partial C_m}{\partial \frac{\dot{\alpha}\bar{c}}{2V}}$

λ taper ratio, Tip chord/Root chord

A dot above a symbol denotes differentiation with respect to time.

APPARATUS

Wind Tunnel

The tests were made in the jet of the Langley gas dynamics laboratory described in reference 8. This is a blowdown jet exhausting to atmosphere,

[redacted]

with dry air being supplied to the settling chamber at 100° F and at pressures up to 500 lb/sq in. gage. A calibration of the supersonic nozzles used in this investigation indicated a maximum variation in Mach number of ±0.02 in the test regions.

Models

Dimensions of the three wing models tested are given in figure 1(a). The models were constructed of steel, and each model has a constant ratio of maximum thickness to chord of 0.04. The cross section of each model was a symmetrical modified-diamond shape. Side-wall mounting was used, as shown in figure 1(b), and the clearance between the edge of the wing and the side wall was approximately 0.010 inch.

Balance

The balance supporting the model is shown in figures 2(a) and 2(b). It is a free-oscillation balance with the model-support beam attached to the main support with crossed flexure beams. The restoring moment of these beams supplies the spring constant in the system, and strain gages attached to these beams give the angular displacement of the model. Adjustable weights at the end of the model-support beam provide for changing the moment of inertia of the system. A modified loudspeaker was installed to force oscillation of the model, but instrumentation difficulties prevented the obtaining of enough forced-oscillation data for publication. This drive unit remained with the balance during free-oscillations tests but was disconnected electrically.

The circular disk supporting the model is flush with the side wall, with about 0.010-inch clearance on the radius. This disk is attached to the model-support beam in such a manner as to allow adjustment of the angle of attack of the model. The complete balance is enclosed in a vacuum-tight chamber to prevent flow of air into the test section in the region of the model.

Instrumentation

The output of the strain gages attached to the flexure support beams was put into the galvanometer element of a recording oscillograph. Thus, a time history of the displacement of the model was recorded on film moving at the rate of 6 inches per second. Timing lines recorded on the film each 0.01 second give a measure of the frequency of oscillation. A typical record is shown in figure 3.

PROCEDURE

Scope of Tests

The present investigation was made at Mach numbers of 2.96 and 3.92 and at Reynolds numbers per foot of 15×10^6 and 25×10^6 at each Mach number. (Reynolds number range based on mean aerodynamic chord was from 4×10^6 to 12×10^6.) The angle of attack of the model was varied in 2° increments from 0° to 10°. The center of pitching oscillation was varied about 5 percent for each model, being located at a distance from the wing apex of about 90 percent and 95 percent of the mean aerodynamic chord for the delta wings and about 93 percent and 101 percent for the sweptback tapered wing. Oscillation frequencies were about 15 and 28 cycles per second. The corresponding values of reduced-frequency parameter $\frac{\omega\bar{c}}{2V}$ were 0.006 and 0.011 for the sweptback tapered wing, 0.008 and 0.015 for the delta wing of aspect ratio 3, and 0.011 and 0.022 for the delta wing of aspect ratio 2. All data were taken at an amplitude of $\theta = 3^\circ$.

Reduction of Data

The differential equation for the motion of a one-degree-of-freedom mass system with viscous damping and a linear spring constant is

$$I\ddot{\theta} + D\dot{\theta} + K\theta = 0 \tag{1}$$

When the value of the damping is less than the critical damping for the system, the solution of equation (1) can be written as

$$\theta = \theta_0 e^{-\frac{D}{2I}t}\left(\cos \omega t + \frac{D}{2I\omega} \sin \omega t\right) \tag{2}$$

where θ_0 is the value of θ at $t = 0$ and $\omega = \left[\frac{K}{I} - \left(\frac{D}{2I}\right)^2\right]^{1/2}$. With the term $\left(\cos \omega t + \frac{D}{2I\omega} \sin \omega t\right)$ of equation (2) a maximum, the following equation is obtained for the envelope of the maximum values of θ:

$$\theta = \theta_0 e^{-\frac{D}{2I}t} \tag{3}$$

Solving for D gives

$$D = \frac{-2I}{t} \log_e \frac{\theta}{\theta_0} \tag{4}$$

The relationship in equation (4) was used in order to reduce the data in this investigation. A curve was drawn through the maximum values of θ on the recording paper, and values of θ were measured at even time increments. The values of D determined from equation (4) were then plotted against θ, and a faired curve through these points gave the final value of D used. The wind-off value of D was subtracted from the wind-on value in order to obtain the aerodynamic moment that was used to determine the stability derivative $C_{m_q} + C_{m_{\dot{\alpha}}}$.

With the probable errors in measuring the quantities involved, the maximum error in obtaining a particular value of D was estimated to be about ±10 percent; however, fairing a curve through the values of D obtained during a run considerably reduced this error. All final values of D were taken at the same amplitude ($\theta = 3^\circ$) in order to reduce any errors due to the effect of amplitude.

The spring constant K was determined with the use of calibrated weights and an accurate clinometer. The moment of inertia I of the system was determined from the natural frequency and the calibrated spring constant by using

$$\omega = \left(\frac{K}{I}\right)^{1/2} \tag{5}$$

A more accurate expression is

$$\omega = \left[\frac{K}{I} - \left(\frac{D}{2I}\right)^2\right]^{1/2}$$

However, the static value of D was so small as to make the term $\left(\frac{D}{2I}\right)^2$ negligible when compared with $\frac{K}{I}$.

Tests were made in an evacuated chamber in order to determine if there were aerodynamic damping moments in the wind-off values of damping. These tests indicated any aerodynamic damping moments were within the accuracy of the data.

The static pitching-moment coefficient C_{m_α} was determined by two different methods in order to estimate the effect of side-wall boundary layer on the forces measured on the models. The first method was the measurement of the model deflection under wind-on conditions before the oscillatory tests were begun. This gave a static value of C_{m_α}. The second method was the measurement of the displacement of the line for $\theta = 0^\circ$ under wind-on oscillatory conditions relative to the line for $\theta = 0^\circ$ at wind-off conditions. This method gave a value of C_{m_α} that included any inertia effects. The values of C_{m_α} given by the two methods were identical and are shown in figure 4.

While it is not known exactly how the boundary layer on the side wall affects dynamic moments, it is felt the effect was small since the values of C_{m_α} were the same under static and dynamic conditions.

RESULTS AND DISCUSSION

The variation of $C_{m_q} + C_{m_{\dot{\alpha}}}$ with angle of attack is shown for the delta wings in figures 5 and 6 and for the sweptback tapered wing in figure 7. The trend of increasing damping with increased angle of attack is present for all the wings at each Mach number. In general, there is very little change in $C_{m_q} + C_{m_{\dot{\alpha}}}$ with change in α up to $\alpha = 4^\circ$; most of the change occurs for $\alpha > 6^\circ$. This fact is particularly true for the delta wings.

There is no significant change in damping with change in pitching-center location for any of the wings tested. However, the test conditions were such that $d/\bar{c}$ could be varied only a small amount. Thus the change in $C_{m_q} + C_{m_{\dot{\alpha}}}$ predicted by theory could have been obscured by the accuracy of the data.

The effect of change in Reynolds number and aspect ratio on the damping $C_{m_q} + C_{m_{\dot{\alpha}}}$ is within the accuracy of the data. The change in the reduced-frequency parameter $\frac{\omega\bar{c}}{2V}$ does not noticeably affect $C_{m_q} + C_{m_{\dot{\alpha}}}$ for the delta wings; but, for the sweptback tapered wing, increasing $\frac{\omega\bar{c}}{2V}$ considerably decreases the damping. This trend is just opposite to that obtained in reference 7. However, the reduced-frequency parameters in reference 7 were nearer the region of flutter. It is not likely that this trend is due to torsional oscillations since the natural frequency of torsional oscillation for the wing in this report is extremely high and the torsional damping of the material is rather large. One explanation may be that the pressure fluctuations separated the boundary layer in the outboard region of the wing, although it is not apparent how the frequency of oscillation would affect this.

The variation of $C_{m_q} + C_{m_{\dot{\alpha}}}$ with Mach number for the delta wings is shown in figure 8. The decrease in damping with increasing Mach number follows theory; however, the absolute values of damping are about 15 percent below theoretical values.

SUMMARY OF RESULTS

An investigation has been made to determine the damping-in-pitch parameter $C_{m_q} + C_{m_{\dot{\alpha}}}$ for two delta wings and a sweptback tapered wing at Mach numbers 2.96 and 3.92 over a range of Reynolds numbers based on mean aerodynamic chord from 4×10^6 to 12×10^6 and an angle-of-attack range of 0° to 10°. Also varied were the position of the center of rotation and the oscillation frequency. This investigation indicated the following general results:

1. The damping of all wings increased with increasing angle of attack, and the rate of increase in damping was larger at the higher angles of attack.

2. For the delta wings the damping decreased with an increase in Mach number but was about 15 percent below the theoretical value at each Mach number.

3. A change in frequency of oscillation had no effect on the damping of the delta wings; but, for the sweptback tapered wing, increasing the frequency of oscillation decreased the damping.

4. There was no effect of Reynolds number or change in pitching-center location on $C_{m_q} + C_{m_{\dot{\alpha}}}$.

Langley Aeronautical Laboratory,
National Advisory Committee for Aeronautics,
Langley Field, Va., June 20, 1957.

REFERENCES

1. Brown, Clinton E., and Adams, Mac C.: Damping in Pitch and Roll of Triangular Wings at Supersonic Speeds. NACA Rep. 892, 1948. (Supersedes NACA TN 1566.)

2. Ribner, Herbert S., and Malvestuto, Frank S., Jr.: Stability Derivatives of Triangular Wings at Supersonic Speeds. NACA Rep. 908, 1948. (Supersedes NACA TN 1572.)

3. Martin, John C., Margolis, Kenneth, and Jeffreys, Isabella: Calculation of Lift and Pitching Moments Due to Angle of Attack and Steady Pitching Velocity at Supersonic Speeds for Thin Sweptback Tapered Wings With Streamwise Tips and Supersonic Leading and Trailing Edges. NACA TN 2699, 1952.

4. Cole, Isabella J., and Margolis, Kenneth: Lift and Pitching Moment at Supersonic Speeds Due to Constant Vertical Acceleration for Thin Sweptback Tapered Wings With Streamwise Tips - Supersonic Leading and Trailing Edges. NACA TN 3196, 1954.

5. Tobak, Murray: Damping in Pitch of Low-Aspect-Ratio Wings at Subsonic and Supersonic Speeds. NACA RM A52L04a, 1953.

6. Henderson, Arthur, Jr.: Investigation at Mach Numbers of 1.62, 1.93 and 2.41 of the Effect of Oscillation Amplitude on the Damping in Pitch of Delta-Wing—Body Combinations. NACA RM L53H25, 1953.

7. Orlik-Rückemann, Kazimierz, and Olsson, Carl Olof: A Method for the Determination of the Damping-in-Pitch of Semi-Span Models in High-Speed Wind-Tunnels, and Some Results for a Triangular Wing. Rep. No. 62, Aero. Res. Inst. of Sweden (Stockholm), 1956.

8. Moore, John A.: Investigation of the Effect of Short Fixed Diffusers on Starting Blowdown Jets in the Mach Number Range From 2.7 to 4.5. NACA TN 3545, 1956.

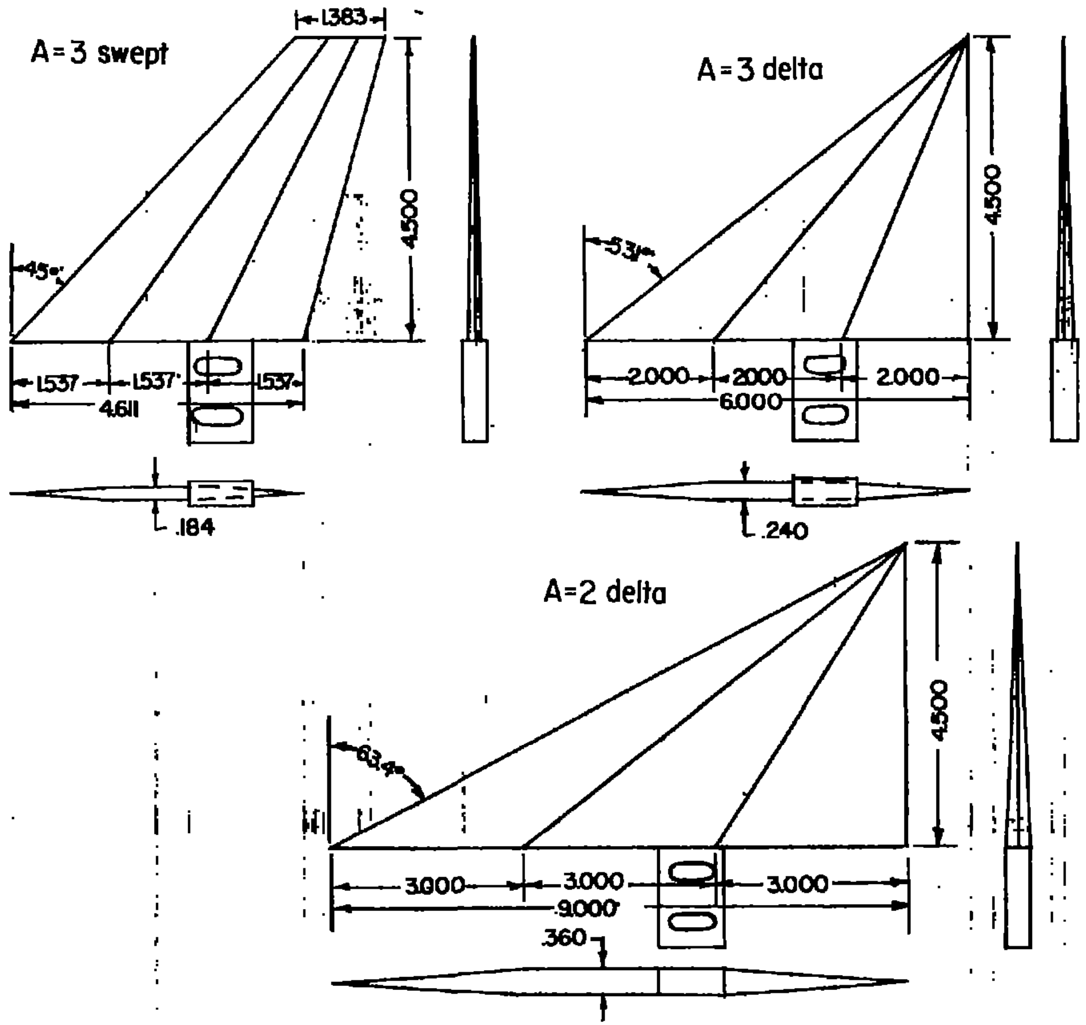

(a) Schematics of wing models tested.

Figure 1.- Wing models tested. Linear dimensions are in inches.

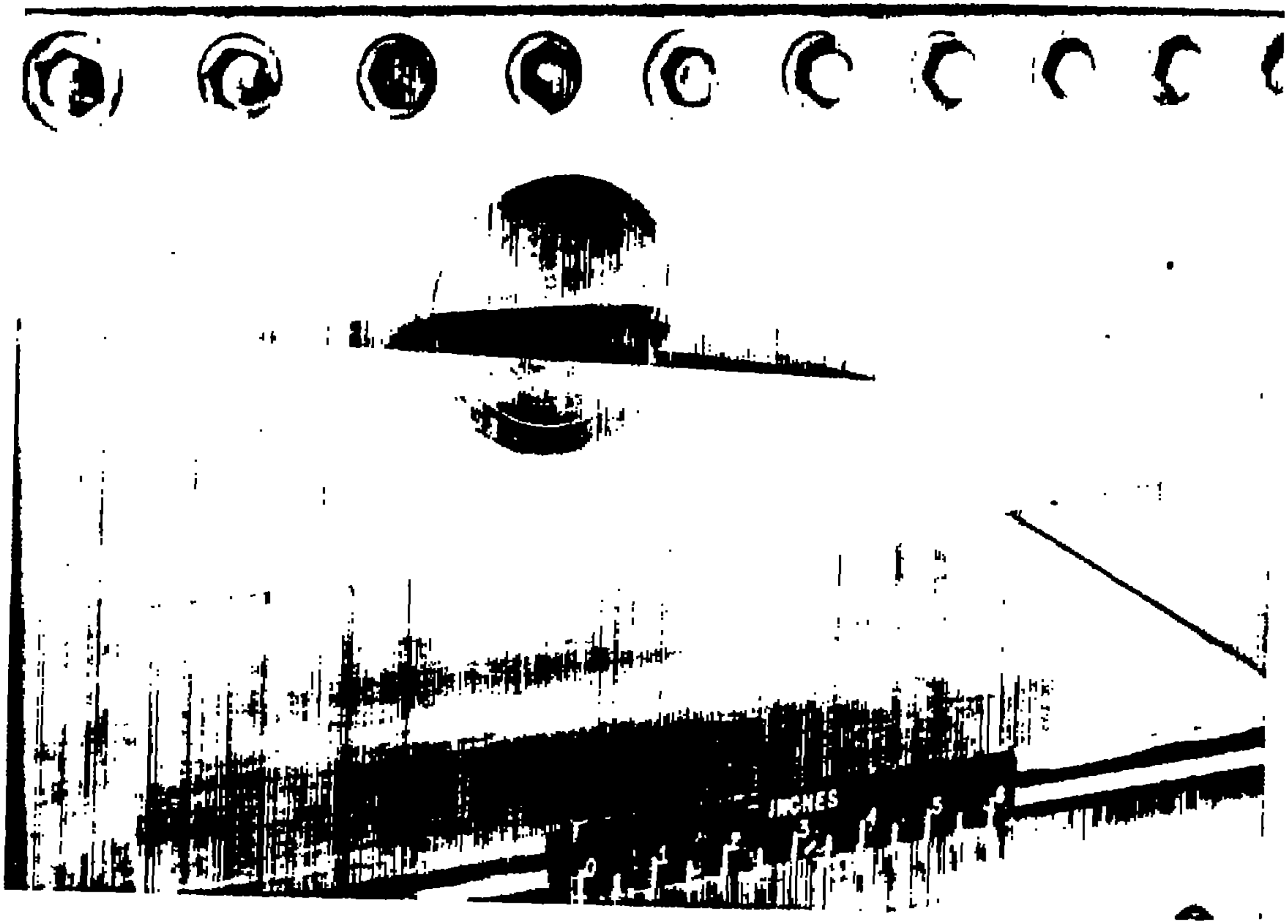

(b) Typical installation of model in tunnel. L-93600

Figure 1.- Concluded.

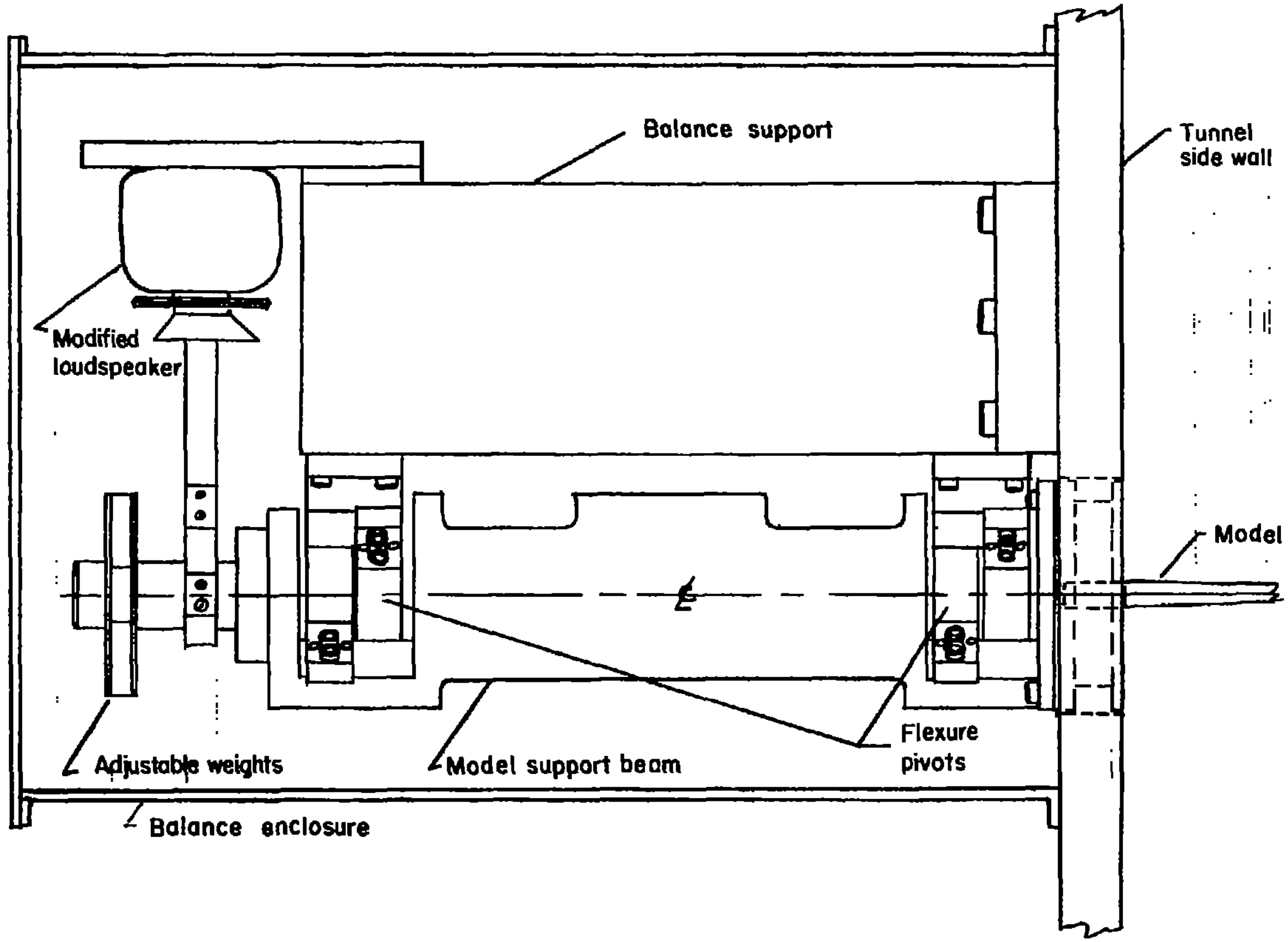

(a) Schematic side view of balance.

Figure 2.- Balance system.

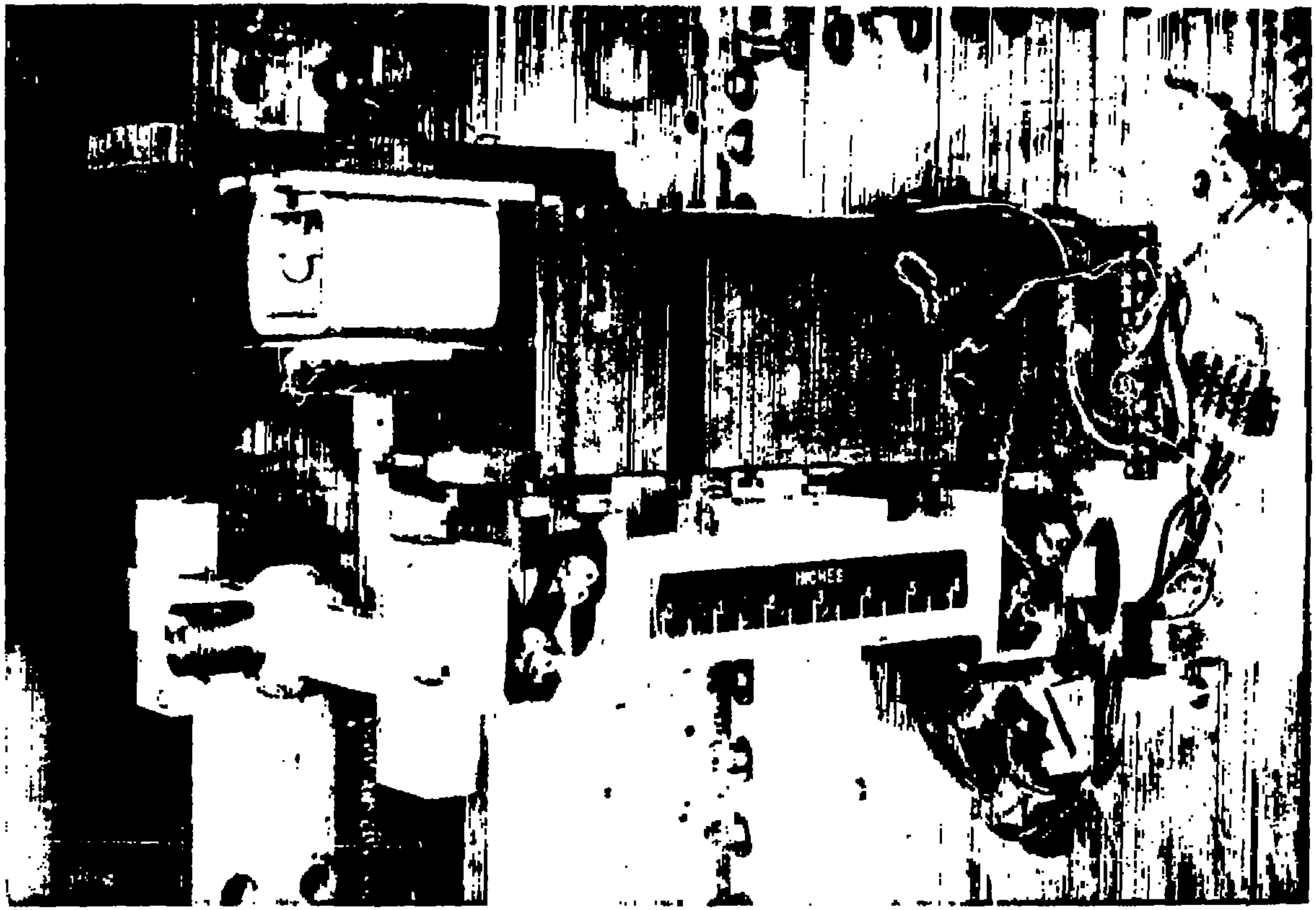

(b) Balance installed on tunnel side wall. L-93601

Figure 2.- Concluded.

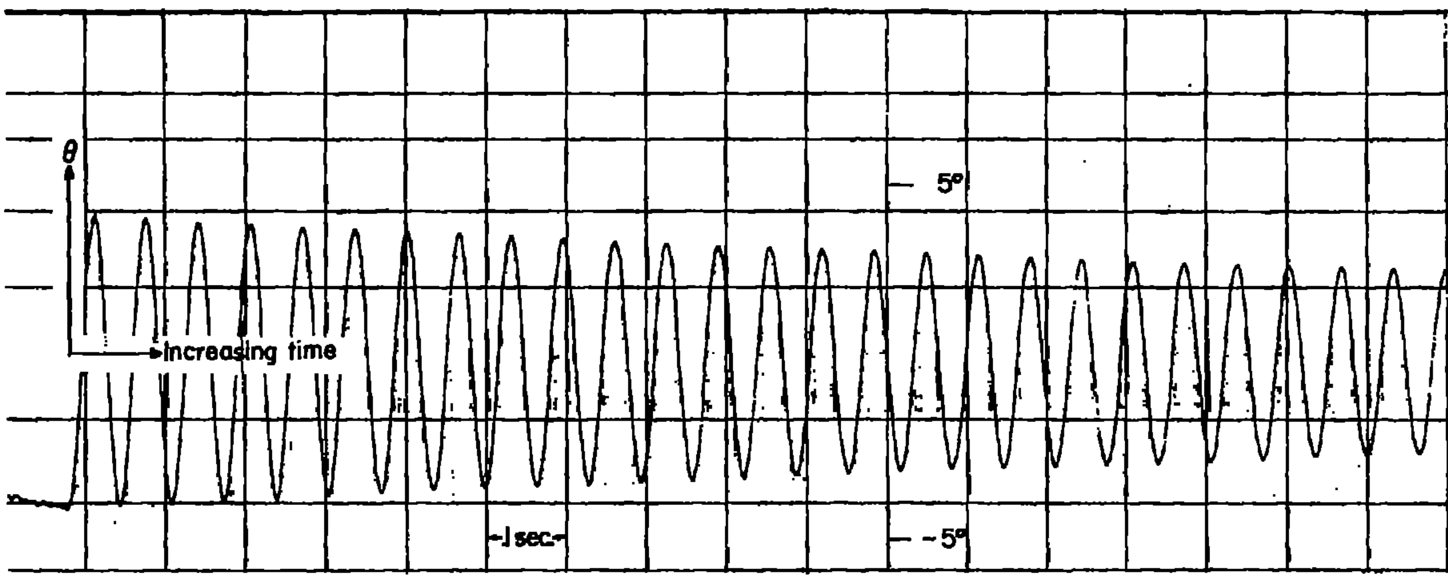

Figure 3.- Typical oscillation record.

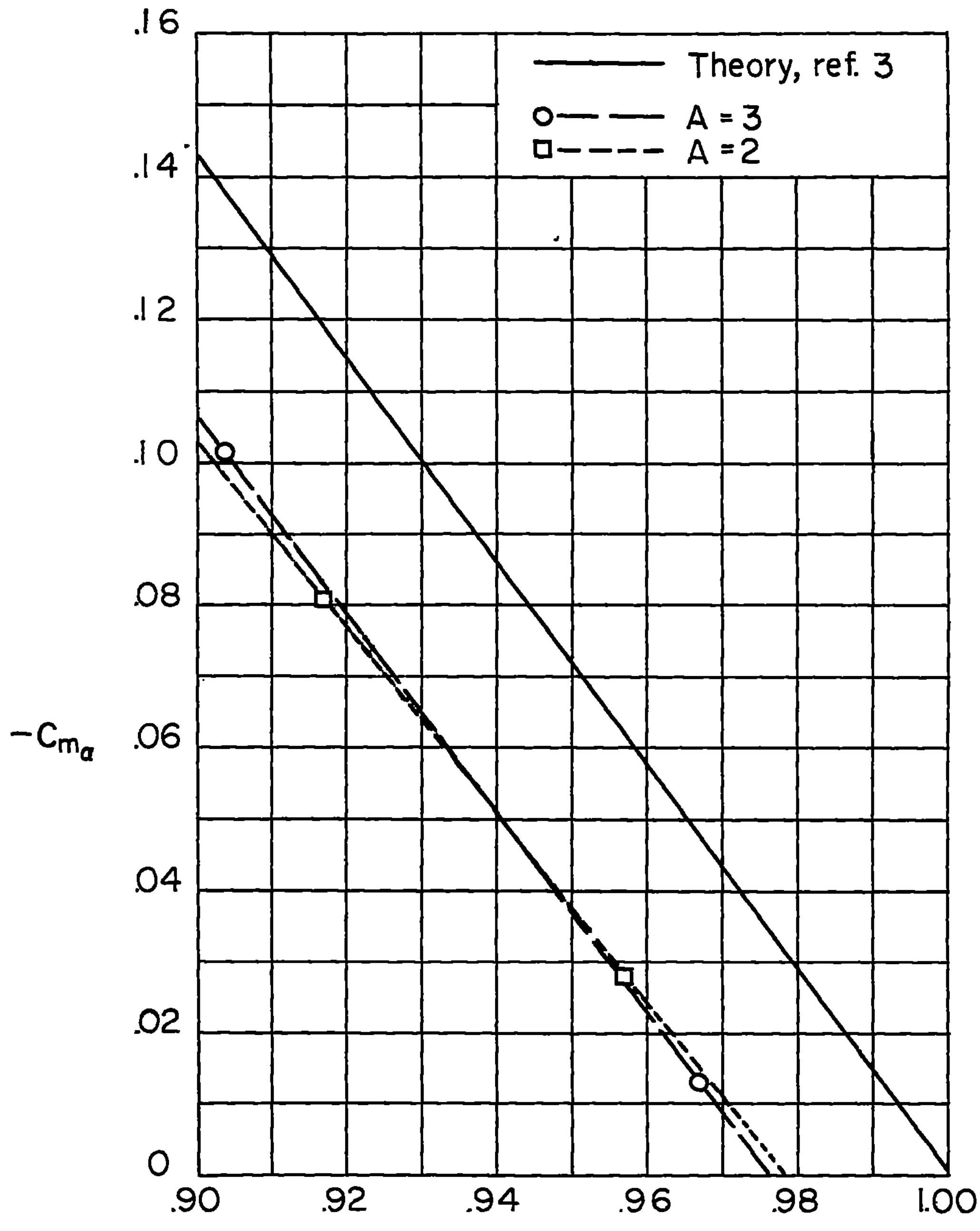

(a) Delta wing at $M = 2.96$.

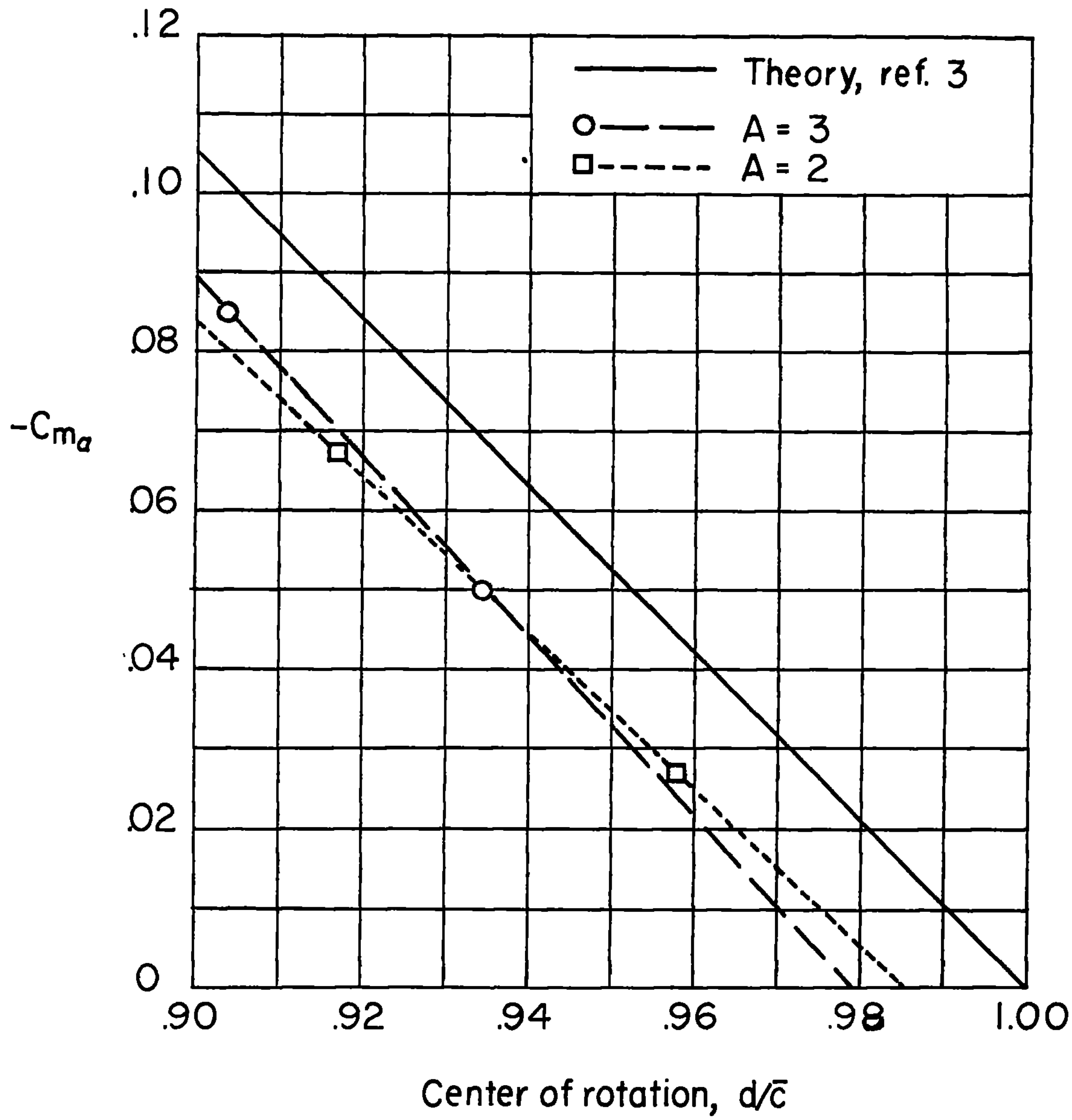

(b) Delta wing at M = 3.92.

Figure 4.- Continued.

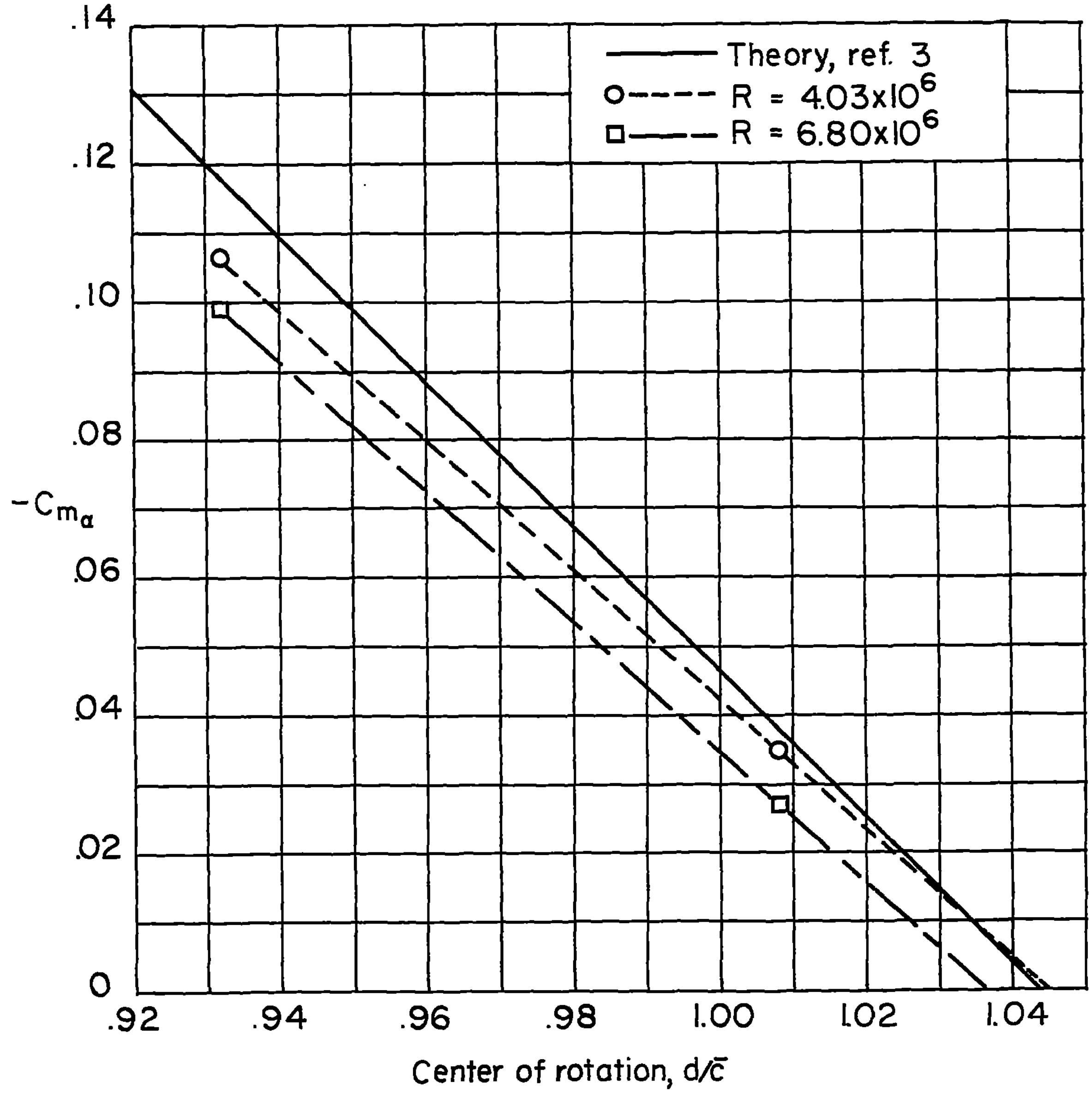

(c) Sweptback tapered wing at $M = 3.92$.

Figure 4.- Concluded.

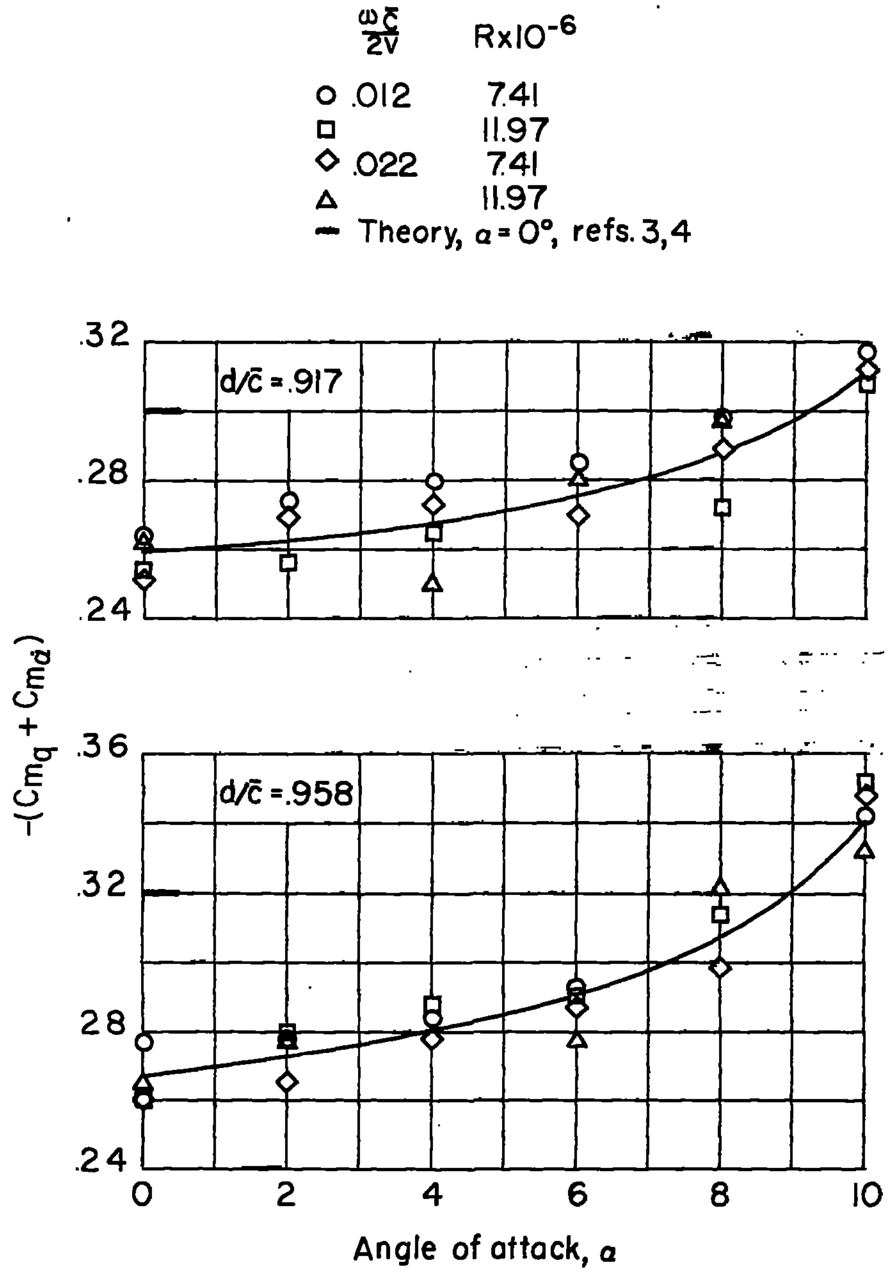

(a) M = 2.96.

Figure 5.- Variation of $C_{m_q} + C_{m_{\dot{\alpha}}}$ with angle of attack for delta wing. A = 2.

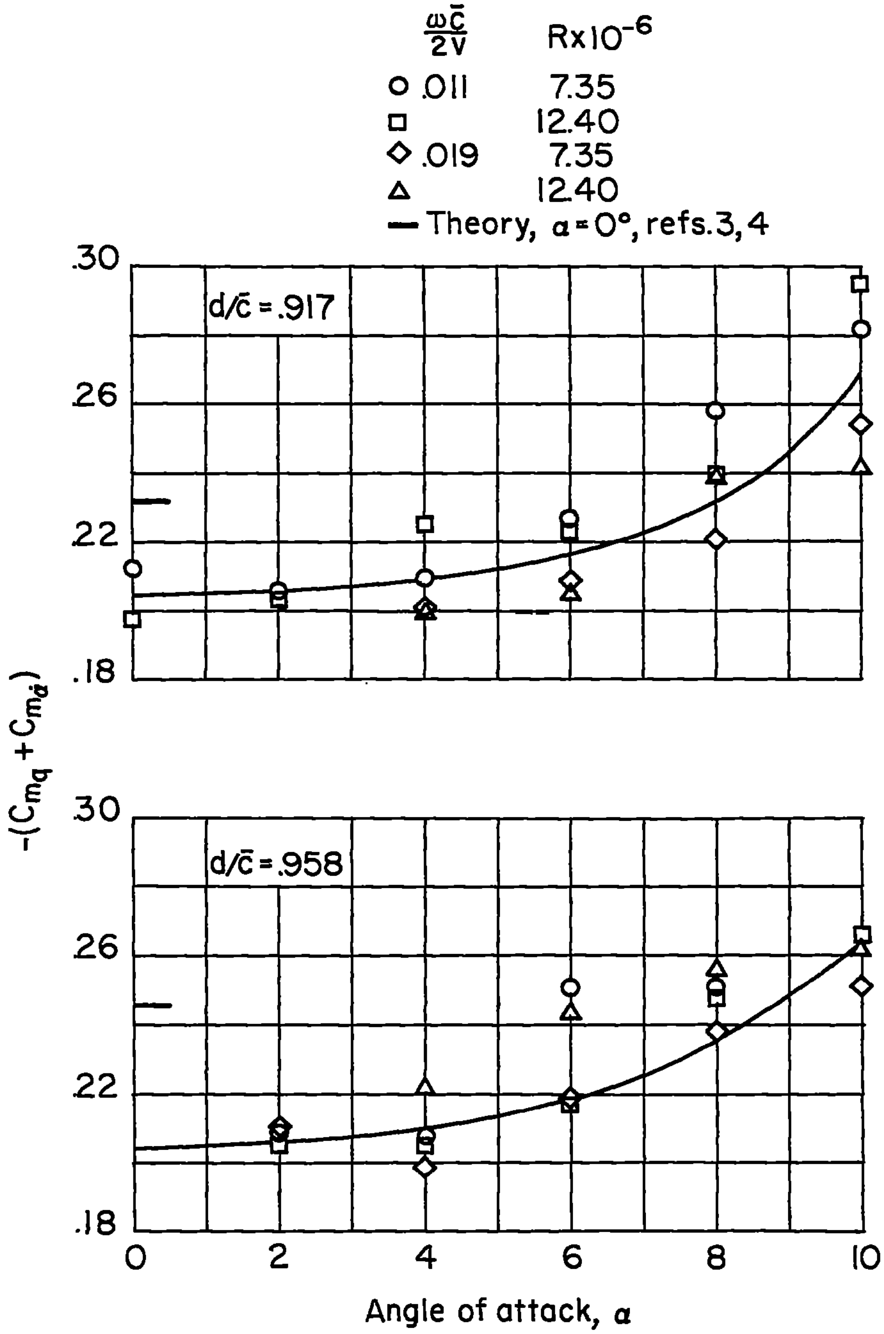

(b) M = 3.92.

Figure 5.- Concluded.

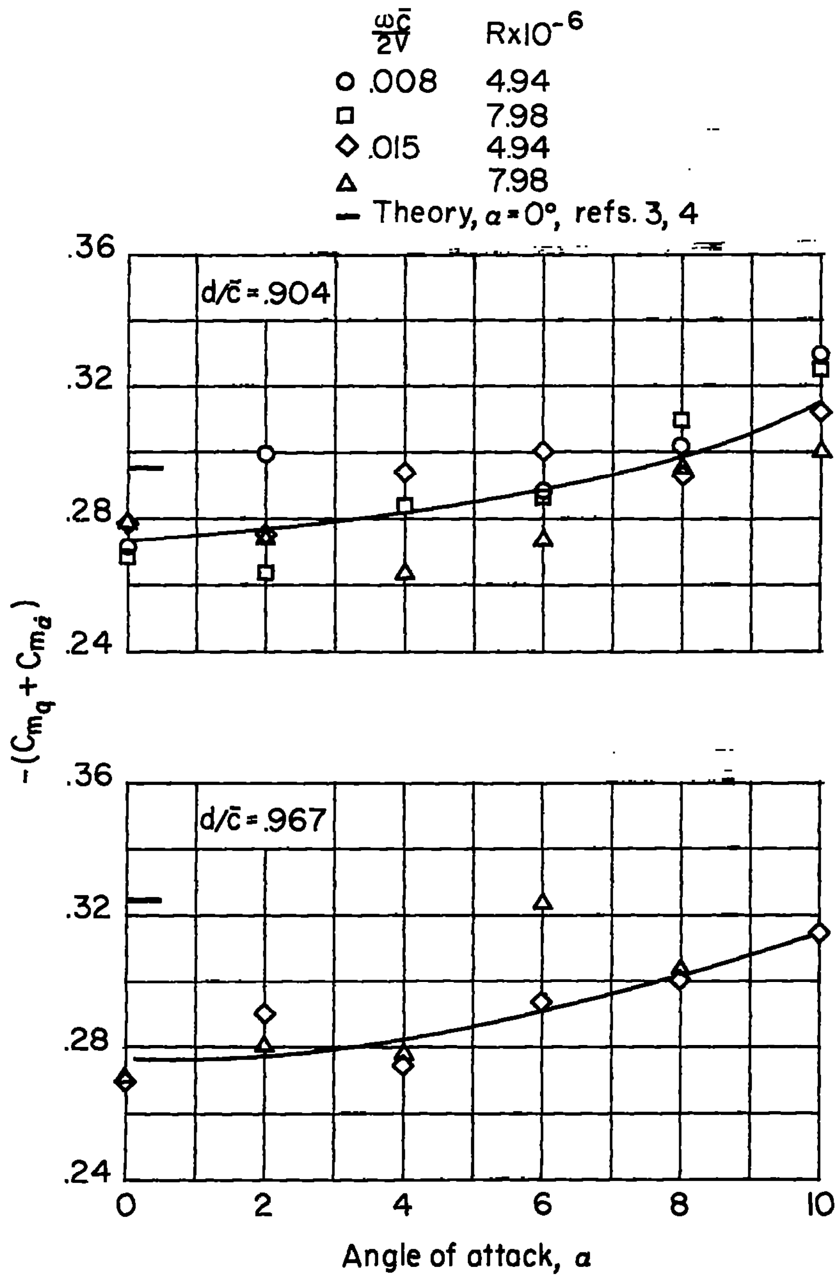

(a) M = 2.96.

Figure 6.- Variation of $C_{m_q} + C_{m_{\dot{\alpha}}}$ with angle of attack for delta wing. A = 3.

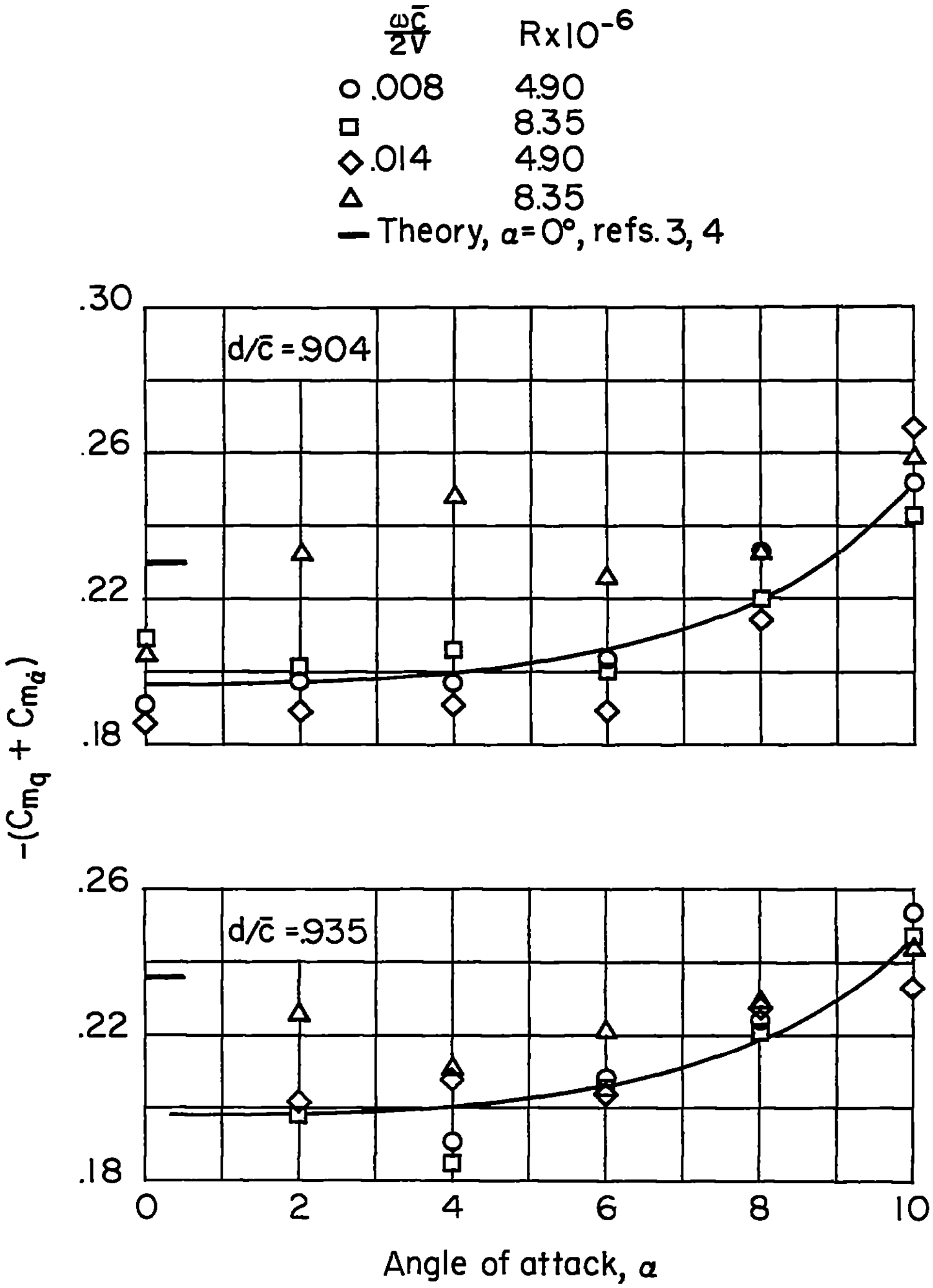

(b) M = 3.92.

Figure 6.- Concluded.

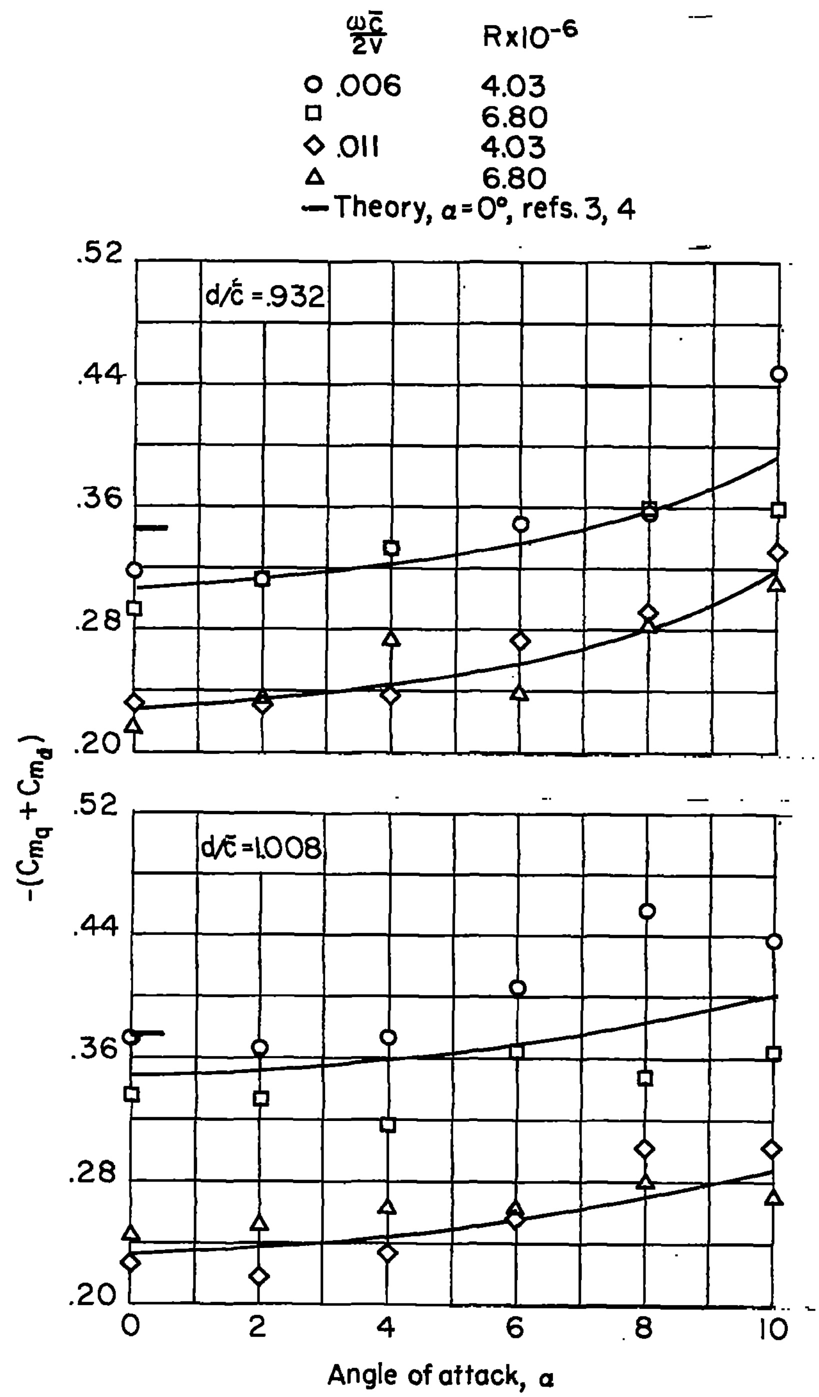

Figure 7.- Variation of $C_{m_q} + C_{m_{\dot{\alpha}}}$ with angle of attack for sweptback tapered wing at M = 3.92. A = 3.

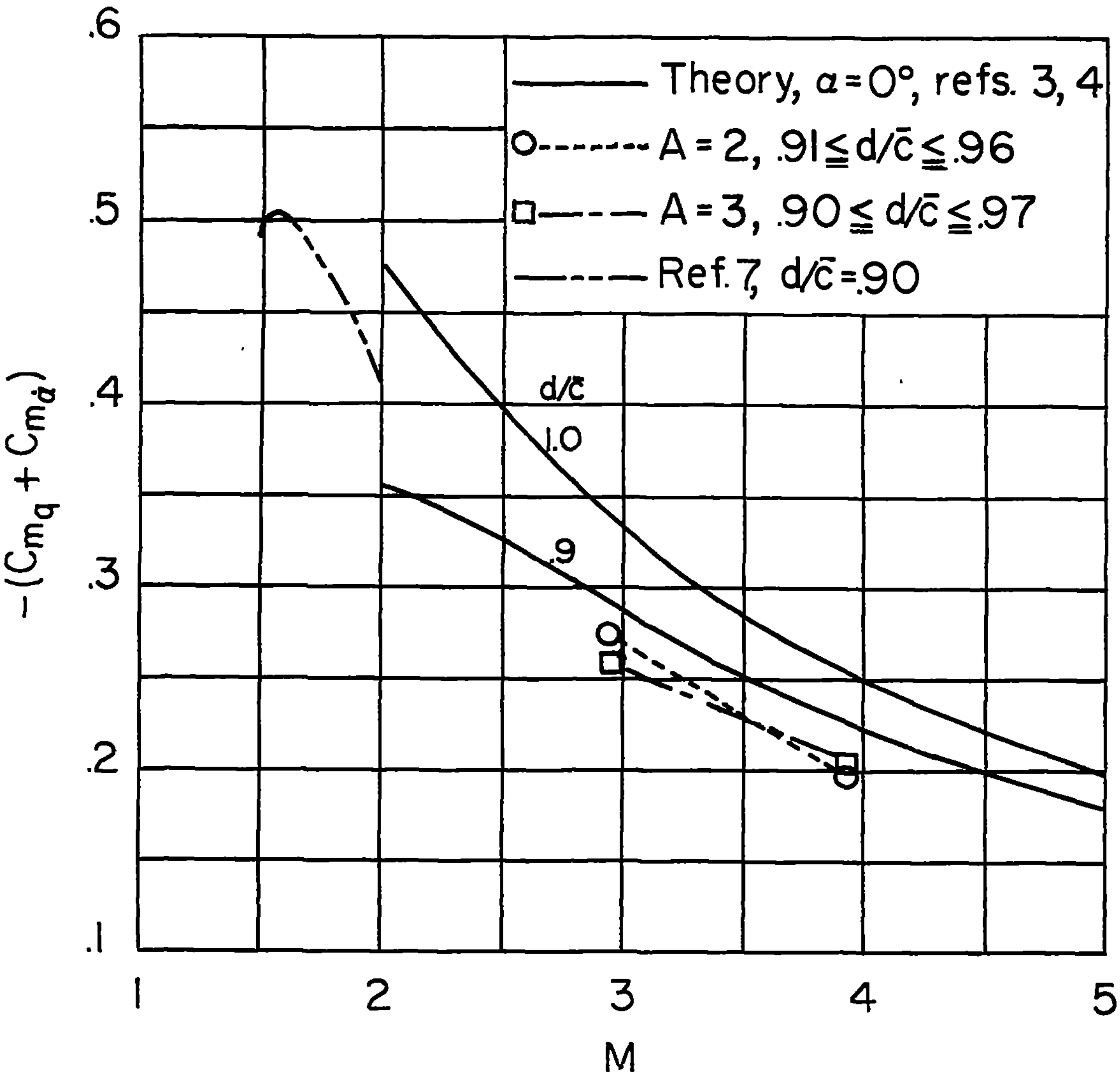

Figure 8.- Variation of $C_{m_q} + C_{m_{\dot{\alpha}}}$ with Mach number for delta wings.